The Astrophysical Journal, 669: L49–L52, 2007 November 1

SOLAR FLARE HARD X-RAY EMISSION FROM THE HIGH CORONA

Säm Krucker,[1] S. M. White,[2] and R. P. Lin[1,3]

Received 2007 August 5; accepted 2007 September 18; published 2007 October 9

ABSTRACT

One of the largest solar hard X-ray (HXR) flares and solar energetic particle (SEP) events recorded by the *Mars Odyssey* mission while orbiting Mars occurred on 2002 October 27 and is related to a very fast (~2300 km s^{-1}) coronal mass ejection (CME). From the Earth, the flare site is 40.4° ± 3.5° behind the solar limb and only emissions from the high corona at least 1.5×10^5 km radially above the main flare site can be seen. Nevertheless, the Earth-orbiting *Reuven Ramaty High Energy Solar Spectroscopic Imager* (*RHESSI*) observed HXR emission up to 60 keV with a relatively flat, nonthermal spectrum (γ between 3 and 3.5) that has an onset simultaneous with the main HXR emission observed above 60 keV by the Gamma-Ray Spectrometer (GRS) orbiting Mars. While GRS records several smaller enhancements after the main peak, the high coronal source observed by *RHESSI* shows a long exponential decay ($\tau = 135 \pm 5$ s) with progressive spectral hardening. The emissions from the high corona originate from an extended source (~1.5×10^5 km in diameter) that expands (390 ± 70 km s^{-1}) and moves upwards (750 ± 80 km s^{-1}) in the same direction as the CME. These observations reveal the existence of energetic electrons in the high corona in closed magnetic structures related to the CME that are accelerated at the same time as the main energy release in the flare. Although the number of energetic electrons in the high corona is only a small fraction of the total accelerated electrons, about 10% of all electrons in the high coronal source are nonthermal (>10 keV).

Subject headings: Sun: flares — Sun: particle emission — Sun: X-rays, gamma rays

1. INTRODUCTION

Particle acceleration is observed to be efficient in solar flares and coronal mass ejections (CME), producing energetic electrons up to hundreds of MeV and ions up to several GeV. Furthermore, the accelerated particles often contain a large fraction of the total released energy. The acceleration mechanisms, however, are not understood. X-ray observations provide diagnostics of flare-heated thermal plasma and flare-accelerated nonthermal electrons via the electron bremsstrahlung mechanism. Thermal emission generally dominates below ~20 keV and is most prominent from flare loops reaching maximum heights of up to 15% of the solar radius. At higher energies, bremsstrahlung emission from nonthermal flare-accelerated electrons with much harder (flatter) spectra is seen. Since nonthermal bremsstrahlung depends on the ambient plasma density, emission strongly increases in the transition region and is therefore most prominent from footpoints of flare loops, but fainter emission is also seen sometimes from the corona (Tomczak 2001; Battaglia & Benz 2006; Krucker & Lin 2007). The limited dynamic range of X-ray observations makes it generally difficult to detect faint emission besides the main thermal component from flare loops and the nonthermal footpoint sources. Partially limb-occulted flare observations, however, have been used to investigate faint emissions from the corona. HXR emissions have been reported from flares with occultation heights up to 0.3 $R_\odot$ (i.e., flare location is 40° behind the solar limb). These emissions originate well above the main thermal flare loops, show a flat spectrum, and contain ~0.1%–1% of the total flare energy (Hudson 1978; Kane et al. 1992; Hudson et al. 2001). Furthermore, fast source motions with velocities similar to that of the CME are observed (Hudson et al. 2001), suggesting that the HXR emission is produced by nonthermal electrons in a moving magnetic structure.

In this Letter, an event with an occultation height of 0.3 $R_\odot$ observed by the *Reuven Ramaty High Energy Solar Spectroscopic Imager* (*RHESSI*; Lin et al. 2002) is presented. *RHESSI* provides for the first time high-resolution imaging spectroscopy that allows us to obtain physical parameters of thermal and nonthermal emissions from coronal sources observed well above the main flare loops.

2. OBSERVATIONS AND DATA ANALYSIS

The Gamma-Ray Spectrometer (GRS; Boynton et al. 2004) on *Mars Odyssey* (Saunders et al. 2004) detected a very intense solar HXR flare on 2002 October 27 (Fig. 1) peaking at 22:53:24 UT (all times from observations at Mars given in this Letter are corrected for the longer travel time of electromagnetic radiation from the Sun to Mars compared to Earth to enable direct comparison with near-Earth observations). The GRS peak count rate for this flare is larger by 50% than for the X7.1 flare on 2005 January 20 and only about a factor of 2 smaller than the >X17 flare on 2003 October 28, suggesting that the 2002 October 27 flare is likely a very large X-class flare. *Mars Odyssey* also recorded a very large solar energetic particle (SEP) event related to the 2002 October 27 flare, while no SEP event is reported near Earth. At the time of the flare, Mars and Earth were separated by 138° and the nominal Parker spiral connecting Mars to the Sun suggests a flare location ~40° behind the solar limb seen from Earth. *SOHO* LASCO observations report an extremely fast (~2300 km s^{-1}) and massive (~1×10^{16} g) coronal mass ejection (CME) originating from the backside of the Sun (Yashiro et al. 2004). The CME liftoff time is difficult to approximate due to the poor coverage of the CME at low altitudes (the first LASCO image is taken when the CME is already at 7 $R_\odot$), and linear extrapolations give liftoff times a few minutes before the onset of the HXR flare seen by GRS. Both the origin of the CME and the Parker spiral connection between Mars and the Sun suggest that the

[1] Space Sciences Laboratory, University of California, Berkeley, CA 94720-7450; krucker@ssl.berkeley.edu.
[2] Department of Astronomy, University of Maryland, College Park, MD 20742.
[3] Department of Physics, University of California, Berkeley, CA 94720-7300.

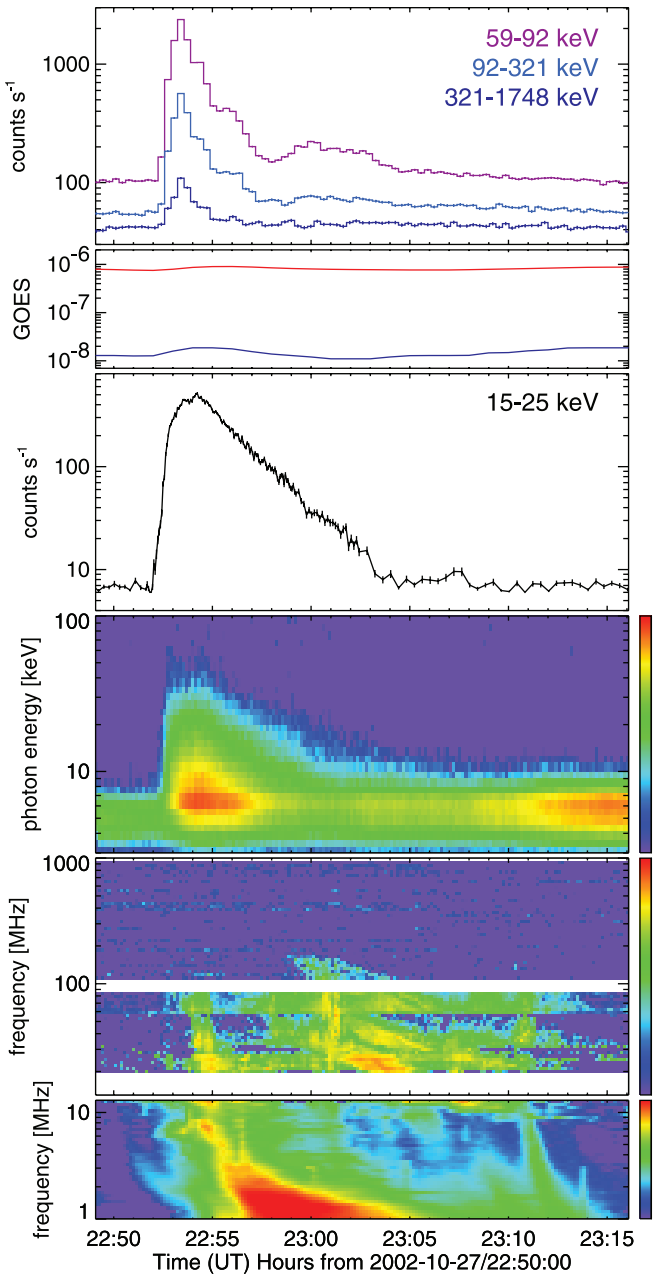

FIG. 1.—Time profile of the 2002 October 27 event in X-rays and radio waves. From top to bottom the panels show (1) GRS hard X-ray time profiles seen from Mars, (2) *GOES* soft X-ray flux seen from Earth, (3) a *RHESSI* 15–25 keV time profile seen from Earth, (4) a *RHESSI* HXR spectrogram, (5) radiospectrogram observations from Culgoora Observatory and from (6) *Wind* WAVES. *RHESSI* X-ray emissions below 10 keV seen before 22:52 UT and after 23:00 UT are not related to the flare occurring behind the limb, but originate from two different active regions on the disk (AR 10162 and AR 10175).

flare occurs in AR 10180. Extrapolating flare locations within AR 10180 from later times when AR 10180 is on the disk from Earth view suggests that AR 10180 was at 40.4° ± 3.5° behind the eastern limb at the time of the flare. Seen from Earth, this corresponds to a radial occultation height of 300″ ± 65″ [(2.2 ± 0.5) × 10^5 km], with extreme values between 200″ and 450″. With such large occultation heights, not only HXR footpoints but also the main thermal flare loops are expected to be occulted. EIT images indeed only show coronal dimming after the flare onset, but do not show flare loops.

Radio observations from Earth from the Culgoora Observatory (above 40 MHz) and from space from *Wind* WAVES (Bougeret et al.1995) show complex emissions such as are typical of large SEP-producing events, with type III bursts (most prominent from 22:52:30 to 22:55:00 UT below ~100 MHz), fundamental and harmonic type II emissions (harmonic emission starting at 22:58:38 UT around 200 MHz), and more complex features possibly including a type IV burst (Fig. 1). The escape of radio emission from the flare site to Earth without absorption along the way indicates an overdense emission region without dense foreground plasma along the line of sight toward Earth. No radio emissions are seen above 200 MHz (and no fundamental emission above 100 MHz) most likely because of limb occultation, suggesting a plasma density at the lowest altitude visible from Earth of the order of 10^8 cm^{-3}.

Despite the flare location behind the solar limb, observations from Earth show clear signals related to the HXR flare seen on Mars (Fig. 1). The *GOES* soft X-ray light curves show a small B2 class event (after subtracting the pre-event background of B8) with an onset roughly simultaneous with the main HXR emission seen from Mars. *RHESSI* detects temporally correlated HXR emissions that are unusually strong for a B-class flare and are seen up to ~60 keV (Fig. 1). The HXR emissions seen by *RHESSI* (<60 keV) and GRS (>60 keV) show similar onsets and rise until the main peak at 22:53:15 UT (the *RHESSI* emission rises a few seconds earlier, but the true onset of the GRS time profiles is likely hidden in the noise of the background). Afterward, the time profiles differ and *RHESSI* shows a long exponential decay (τ = 135 ± 5 s) while GRS observes several minor peaks that are more than an order of magnitude weaker than the main peak. The peak in the *RHESSI* HXR emission correlates well with the period of the type III radio bursts, but not with the type II burst that does not start until around 22:59 UT toward the end of the HXR decay.

2.1. *HXR Imaging*

RHESSI is not a direct imaging system, but uses rotation modulated collimators that store the imaging information in the time profiles (Hurford et al. 2002). Imaging in the thermal and nonthermal range show sources at the eastern limb at the latitude of AR 10180 (Fig. 2). Only the coarsest two collimators show significant modulations in the X-ray flux, implying that the finer collimators have grid spacings much smaller than the source size. From the ratio of modulated to unmodulated counts, a source size can be estimated (assuming a Gaussian source distribution). At the onset of the event, a large source (~200″) is seen at both the 3–7 keV and 10–30 keV energy ranges (Fig. 2). This indicates that right after the onset of the HXR event, the flare is injecting energetic electrons into large altitudes above the flare site. After the peak of the HXR event, the source starts expanding and moves upward in the same direction as the CME. For the last part of the exponential decay (after 23:00:00 UT) no modulation is observed even for the coarsest collimator as the source becomes too large to be imaged by *RHESSI*. The derived expansion speed is 390 ± 70 km s^{-1} and the upward motion of the source is about twice as fast (750 ± 80 km s^{-1}). This is significantly lower than the speed of the CME front (~2300 km s^{-1}), but similar to the speed of the filament seen behind the CME front. The filament is best seen in the LASCO images taken after 23:50 UT and moves at ~1000 km s^{-1}.

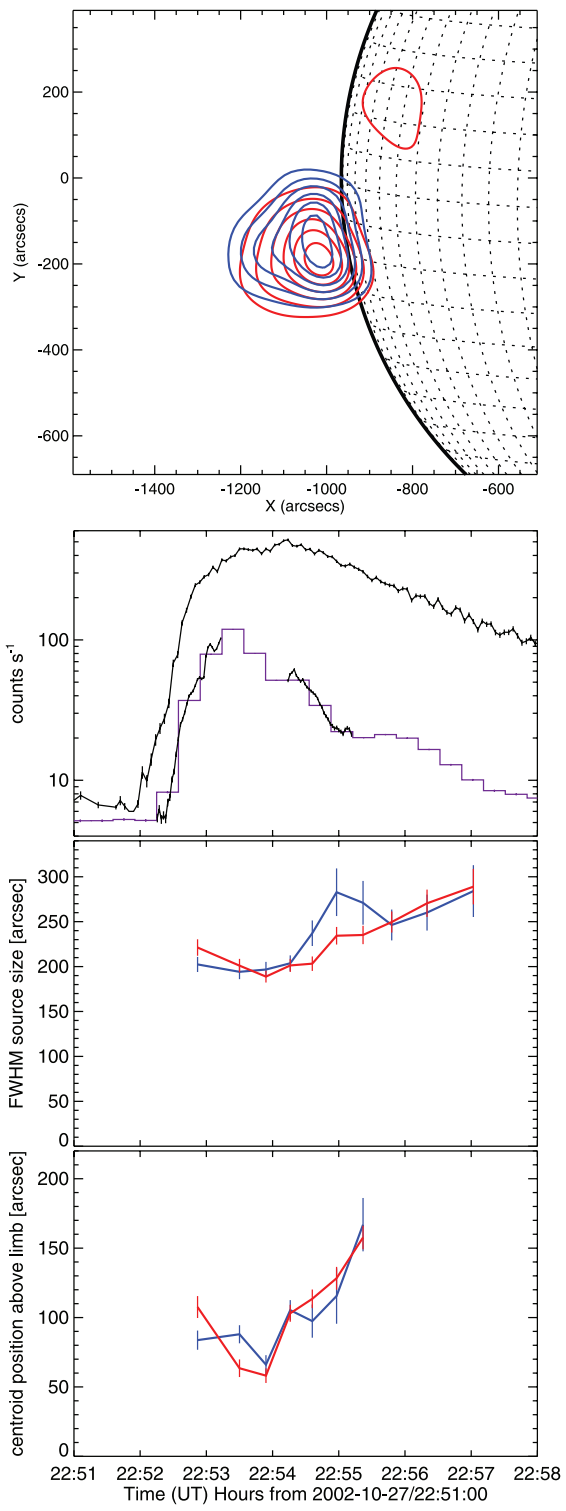

FIG. 2.—*RHESSI* imaging results. *Top*: *RHESSI* flare-averaged imaging in the thermal range (3–7 keV; *red contours*) and nonthermal range (10–30 keV; *blue contours*) reveal large sources just above the limb. The *RHESSI* CLEAN algorithm is used to reconstruct these images (clean beam is 135″), and the contour levels are 15, 30, 45, 60, 75, and 90 percent. The thermal emission on the disk is from AR 10717 and is already present before the limb flare occurs. *Three lower panels*: Temporal evolution of the X-ray source size and centroid position in the thermal (*red*) and nonthermal (*blue*) range. For comparison, the top panel shows the 15–25 keV *RHESSI* count rates (*black*) and the 59–92 keV time profile from GRS on *Mars Odyssey* (the 20 s averaged data is shown in purple and the high time resolution burst data in black; both GRS count rates are divided by 20 for a clearer representation).

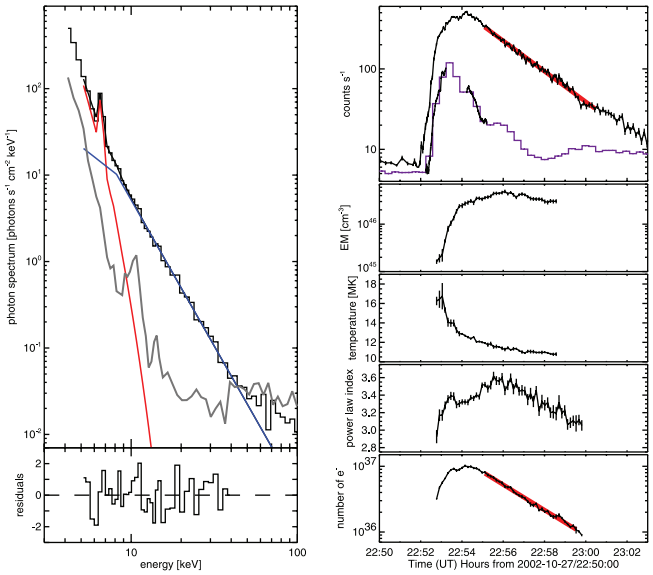

FIG. 3.—Temporal evolution of the spectral parameters. *Left*: Observed photon spectrum (*black*) during the exponential decay (22:56:48 to 22:57:00 UT) with the thermal fit in red and a broken power law fit in blue. The gray line represents the background emission, and the lower panel shows the normalized residuals of the fit. *Right*: The top panel shows the 15–25 keV *RHESSI* time profiles (*black*) and the 59–92 keV time profile from GRS (same as in Fig. 2). The decay of the *RHESSI* HXR emission is fitted with an exponential with $\tau = 135 \pm 5$ s (*red*). The lower panels show emission measure, temperature, power-law index, and instantaneous number of electrons above 10 keV, respectively.

2.2. *Spectral Fitting*

Spectral fitting for this event is made difficult by time variations in the background emissions. At low energies, thermal emissions from active regions on the solar disk are increasing during the event, making thermal fits after 22:58:30 UT unreliable. At higher energies, magnetospheric particles produce time variations in the nonsolar background. However, at times before 23:00:00 UT, flare emissions clearly dominate below 40 keV. A thermal and a broken power law with a fixed power law index of -1.5 below the break represents the data well (Fig. 3). Thermal emissions dominate below 8 keV and show hottest temperatures initially with slowly decreasing temperatures afterward. The emission measures are rather low even at the peak ($\sim 5 \times 10^{46}$ cm^{-3}), and, together with the derived source sizes from imaging, the density of the thermal source becomes of the order of 1×10^{8} cm^{-3} (for a filling factor of unity), the same order of magnitude as inferred from radio observations. The thermal source contains about 1×10^{38} electrons with an energy content of 1×10^{30} erg. Above 10 keV, the power law dominates with a rather hard spectrum (indices between 3 and 3.5). These values are comparable to HXR footpoint spectral indices seen in large flares (Saint-Hilaire et al. 2007), and are flatter than most coronal HXR emissions (Krucker & Lin 2007), but not as flat as some of the coronal HXR emission seen in giant flares (Krucker et al. 2007). During the exponential decay of the HXR emission the spectral index is progressively hardening from ~3.5 to ~3. At the peak, the instantaneous number of nonthermal electrons above 10 keV is of the order of 10^{37} (Fig. 3, *bottom*) and is about 10% (a remarkably large fraction) of the total population of electrons in the X-ray source. The total energy of the electrons present at the peak gives a lower limit for the total energy in nonthermal electrons of 2×10^{29} erg. For further energy estimates, model

assumptions have to be made. Since the density in the X-ray source is rather low ($\sim 10^8$ cm^{-3}), the thick-target approximation can only be applied for integration times longer than the collisional loss time (typically several minutes). Assuming that escape of electrons can be neglected (i.e., all electrons are trapped within the X-ray source), the thick-target approximation can be applied for the event-averaged spectrum giving a total energy in nonthermal electrons above 10 keV of 1×10^{30} erg. Spectral comparison between *RHESSI* and GRS observations is not straightforward and will be published later.

Microwave observations taken by the Nobeyama Radio Polarimeter show temporally related emission, and images made at 17 GHz with the Nobeyama Radioheliograph confirm that this emission, while very faint, originates from the same location as the hard X-ray emission. The microwave emission has a spectrum decreasing with frequency above 1 GHz as expected for synchrotron emission from nonthermal electrons, with a power-law index in the range 1.3–1.7. The observed slope corresponds to an electron energy spectral index of 2.8–3.3, and is to within the uncertainties the same as that derived from the HXR observations assuming thin-target emission. Assuming that the same electron population produces both the radio and HXR emission, we can use the *RHESSI*-derived number of nonthermal electrons to determine the magnetic field strength in the radio source, and find that it needs to be of order 1 G.

3. DISCUSSION AND SUMMARY

HXR observations of a solar flare occurring 40° behind the limb reveal the existence of nonthermal flare accelerated electrons in an extended ($\sim 200''$) source about $300''$ radially above the main flare site. The energetic electrons seen in the high corona are accelerated at the same time as the main electron acceleration occurs, but additionally show an exponential decay on a timescale of 135 ± 5 s. This timescale is similar to the collisional loss time of ~25 keV electrons in a plasma with densities of the order of 10^8 cm^{-3}, suggesting that the exponential decay could be explained by collisional losses alone without any further accelerations. To make this work, the nonthermal electrons needed to be trapped in the source as the transit time through the source is only of the order of 2 s. Detailed modeling including spectral inversion is needed to test this hypothesis.

The HXR source is observed to expand in time and also moves away from the Sun, in a fashion similar to the event reported by Hudson et al. (2001), although in this case the HXR source is much larger. Timing, direction, and speed of motion suggest that the nonthermal electrons producing the observed HXR emission are trapped on magnetic field lines related to the CME. The presented findings are in agreement with earlier reports of HXR emission from the high corona (Hudson 1978; Kane et al. 1992; Hudson et al. 2001), suggesting that high coronal emission from solar flares is common, but difficult to observe. The preliminary results of a statistical survey of fast (>1500 km s^{-1}), backside CMEs with good *RHESSI* coverage indeed reveal that all eight events with flare sites occulted between 20° and 50° show HXR emission from the high corona.

The work was supported by NASA contracts NAS5-98033 and NNG05-GI91G. We would like to thank the *Mars Odyssey* team for making their data products available online. S. K. would also like to thank Simon P. Plunkett for organizing a session on "Shocks in the Corona" at the SHINE workshop 2006 that triggered this work.

REFERENCES

Battaglia, M., & Benz, A. O. 2006, A&A, 456, 751
Bougeret, J.-L., et al. 1995, Space Sci. Rev., 71, 231
Boynton, W. V., et al. 2004, Space Sci. Rev., 110, 37
Hudson, H. S. 1978, ApJ, 224, 235
Hudson, H. S., Kosugi, T., Nitta, N. V., & Shimojo, M. 2001, ApJ, 561, L211
Hurford, G. J., et al. 2002, Sol. Phys., 210, 61
Kane, S. R., McTiernan, J., Loran, J., Fenimore, E. E., Klebesadel, R. W., & Laros, J. G. 1992, ApJ, 390, 687
Krucker, S., Hurford, G. D., Shih, A. Y., & Lin, R. P. 2007, ApJ, submitted
Krucker, S., & Lin, R. P. 2007, ApJ, submitted
Lin, R. P., et al. 2002, Sol. Phys., 210, 3
Saint-Hilaire, P., Krucker, S., & Lin, R. P. 2007, Sol. Phys., submitted
Saunders, R. S., et al. 2004, Space Sci. Rev., 110, 1
Tomczak, M. 2001, A&A, 366, 294
Yashiro, S., Gopalswamy, N., Michalek, G., St. Cyr, O. C., Plunkett, S. P., Rich, N. B., & Howard, R. A. 2004, J. Geophys. Res., 109, 7105